The Astrophysical Journal Supplement Series, 148:583–592, 2003 October

MEASUREMENTS AND CALCULATIONS OF PHOTOIONIZATION CROSS SECTIONS OF MULTIPLY CHARGED IONS IN GROUND AND METASTABLE STATES ALONG THE ISONUCLEAR SERIES OF OXYGEN: O^{2+} TO O^{4+}

J.-P. Champeaux,[1] J.-M. Bizau,[2] D. Cubaynes,[2] C. Blancard,[1] S. Nahar,[3] D. Hitz,[4] J. Bruneau,[1] and F. J. Wuilleumier[2]

Received 2003 January 7; accepted 2003 May 22

ABSTRACT

In this paper, we present the first absolute measurements for photoionization of multiply charged oxygen ions: O^{2+} and O^{3+} in the ground state and in several metastable states, as well as relative data for O^{4+}. Multiconfiguration Dirac-Fock and relativistic ***R***-matrix calculations were performed and are tested here by comparison with experimental results. Our experimental and new theoretical results are also compared with the earlier theoretical data obtained in the ***R***-matrix approximation to calculate photoionization cross sections over part of the isonuclear series of multiply charged oxygen ions.

Subject headings: atomic data — methods: laboratory

1. INTRODUCTION

While the response of ionized matter to photoionizing radiation is an important process in the universe, it has been largely unexplored experimentally until recently (West 2001) because of the difficulty in producing and maintaining high enough densities of singly and multiply charged ions. For many years, theory has been almost the only source of information on resonant and continuum (Reilmann & Manson 1979; Verner et al. 1993) photoionization of ions. Theory, however, has not yet been critically tested, and the few cases where experimental and theoretical data were simultaneously available (Peart & Lyon 1987; Nasreen, Deshmukh, & Manson 1988) demonstrated the great need for accurate photoionization cross section measurements. Such experiments are, e.g., a key point to analyze some of terrestrial and stellar atmosphere data. Although more and more data on singly charged ions are becoming now available (Kjeldsen et al. 1999, 2000; Covington et al. 2001), photoionization cross section measurements for multiply charged ions are still very scarce coming, in particular, from the combined use of electron cyclotron resonance ion sources (ECR) and synchrotron radiation emitted by undulators installed on dedicated storage rings (Bizau et al. 2000, 2001; Oura et al. 2001; Müller et al. 2002).

Multiply charged ions of low-Z elements such as carbon, nitrogen, and oxygen are important species present in the terrestrial atmosphere, in the interstellar medium, as well as in the envelopes of many stars. Among these multiply charged ions, oxygen ions play one of the most important roles as they are involved in many photochemical and collisional reactions. Recently, the experimental photoionization cross section has been obtained for singly charged oxygen ions (Covington et al. 2001; Kjeldsen et al. 2002). Extensive calculations using the ***R***-matrix approximation have been reported and are part of a large database on collisional and radiation properties established within the framework of the Opacity Project (Burke, Lennon, & Seaton 1989; Cunto et al. 1993). More recent ***R***-matrix calculations (Nahar & Pradan 1994; Nahar 1998) have improved the theoretical data available by using a higher number of states to describe the target. In this paper, we present the first absolute measurements for photoionization of multiply charged oxygen ions: O^{2+} and O^{3+} in the ground state and in several metastable states, as well as relative data for O^{4+}. Multiconfiguration Dirac-Fock (MCDF) and relativistic ***R***-matrix calculations were performed and tested here by comparison with experimental results. Our experimental results are also compared with the earlier theoretical data obtained within the framework of the Opacity Project and in the nonrelativistic ***R***-matrix photoionization cross section calculations performed for the whole isonuclear series of multiply charged oxygen ions (Nahar 1998).

2. EXPERIMENTAL

Experiments were carried out on the undulator beamline SU6 at the Super ACO-synchrotron source using an ECR ion source (Bizau et al. 2000, 2001, 2003). Single photoionization of O^{2+}, O^{3+}, and O^{4+} ions were measured using the yield photoion spectroscopy technique, which was first implemented by J. West and his collaborators (Lyon et al. 1986). In short, a monochromatized photon beam was merged over a path length of about 20 centimeters with a 4 kV–accelerated O^{q+} ion beam selected from the beam emitted from the ECR ion source using a Wien filter. Two-dimensional intensity distributions of both photon and ion beams were measured by three sets of translating wire beam profile monitors installed upstream and downstream of the interaction path as well as in the middle of this region. After the interaction with the photon beam, the $O^{(q+1)+}$ ion products were electrostatically separated from the parent O^{q+} beam by using two electrostatic cylindrical analyzers placed in series. A Faraday cup and a multichannel plate array were used to measure the current of parent and product

[1] CEA/DAM Ile-de-France, BP 12, F-91680 Bruyères-le-Châtel, France.

[2] Laboratoire d'Interaction des Rayons X avec La Matière (LIXAM), UMR 8624 du CNRS, Université Paris-Sud, B. 350, and Laboratoire pour l'Utilisation du Rayonnement Electromagnétique (LURE), 91405-Orsay, France.

[3] The Ohio State University, Department of Physics and Astronomy, Columbus, OH 43210.

[4] CEA-Grenoble, Département de Recherche Fondamentale sur la Matière Condensée, 17 rue des Martyrs, 38054 Grenoble Cedex 9, France.

ions, respectively. The photon beam was mechanically chopped to modulate the ion signal so that the contribution from the multiply charged $O^{(q+1)+}$ ions produced by collisions of the parent ions with the residual gases and by photoionization can be separated. A calibrated photodiode was used to measure the absolute intensity of the interacting photon beam.

The absolute photoionization cross section σ is determined at a given photon energy $h\nu$ from

$$\sigma = \frac{S \times q \times v}{(I/\eta e) \times (J/e) \times \varepsilon \times T \times F}$$

where S is the counting rate measured by the channel plates, q is the charge of the target ions, v is the velocity of the ions, determined from the potential applied to the ECRIS, I is the current produced by the photons on the calibrated photodiode, η is the efficiency of the photodiode at the photon energy $h\nu$, e is the charge of the electron, J is the current of incident ions in the Faraday cup, ε is the efficiency of the microchannel plates, T is the transmission of the two analyzers, and F is the form factor.

The efficiency ε is measured by comparing, for several ion velocities, the counting rate on the channel plates with the current produced by the same ion beam in a Faraday cup placed just in front of the channel plates, using a subfemtoampere meter. It has been measured to be constant around a value of 0.71 ± 0.04 over the kinetic energy range 16–41 keV, within the uncertainty of the measurements. The value of T is determined by comparing the currents produced by the same beam in Faraday cups placed after the interaction zone and before the detector. Typical values of T are close to 0.95 ± 0.05. The value F is determined by the overlap between the photon and the incident ion beams, integrated over the length of the interaction zone. It is determined using the profile monitors. The length of the interaction zone is defined by applying a bias (typically 300 V) on this region. In that way, the ions produced outside the interaction zone have a different velocity than the ones produced inside and are then discriminated by the analyzers. The relative accuracy of a single measurement is generally 15% (1 standard deviation), resulting mainly from the uncertainties on F (10%), I (5%), ε (5%), and T (5%), and can reach, in some cases, up to 20%. The accuracy on the final result is improved by repeating the measurements N times. The absolute value of the photoionization cross sections presented here results from the average of N single measurements weighted by their variance s_i^2. The uncertainty on this average s is of the order of $1/(\Sigma 1/s_i^2)^{1/2}$ (Bevington 1969).

The overall validity of our calibration procedure was systematically checked by measuring the photoionization cross section of the He^+ ion, which can be analytically calculated with great accuracy. Within our experimental uncertainty, the measured and calculated cross sections were in very good agreement, giving us confidence in the procedure. More experimental details are given in a separate publication (Bizau et al. 2003).

In our experiment, the choice of the spectral resolution (typically 0.2–0.3 eV) was mainly limited by the need of having a high enough photon beam intensity to interact with the low density (10^4–10^6 ions cm^{-3}) of multiply charged parent ions. Since Super ACO is a second generation storage ring, the intensity of the available photon beam is directly proportional to the product of the width of the entrance and exit slits of the monochromator, thus reducing significantly the brightness of the photon beam.

TABLE 1

Estimated Percentage of Ions in the Ground Term and in the Various Metastable Terms for O^{2+}

Term	Percentage
$1s^2 2s^2 2p^2\ ^3P_{0,1,2}$	80
$1s^2 2s^2 2p^2\ ^1D$	14
$1s^2 2s^2 2p^2\ ^1S$	4
$1s^2 2s 2p^3\ ^5S$	2

Multiply charged O^{q+} ions emitted from the ECR source were in the ground term and in some metastable terms. Identification of all the terms present in the medium and evaluation of the fraction of ions in each metastable term were estimated by comparison of our experimental spectra with synthetic theoretical spectra constructed as a weighted sum of the total (excitation + ionization) photoionization cross sections calculated using the MCDF code for each initial term (see next section). The weighted contribution of each term was optimized to reproduce at best the experimental spectrum in the following way. When jumps are observed in the experimental spectrum at the onset of a direct photoionization cross section corresponding to the opening of either $2p$- or $2s$-continuum channels, the amplitude of this onset was used to determine the weight of the corresponding terms, taking into account the values of the theoretical cross sections at this ionization threshold. In the other cases (^5S term for O^{2+}, ^4P terms for O^{3+}), we used the values of the MCDF resonant photoionization cross section at the top of some well-resolved and intense resonances lines (mainly lines numbered 1 in the figures).

For O^{2+}, 80% of the parent ions were determined to be in the $1s^2 2s^2 2p^2\ ^3P_{0,1,2}$ ground term (ionization threshold at 54.87 eV energy), the percentage of ions determined to be in the $1s^2 2s^2 2p^2\ ^1D$ (ionization threshold at 51.9 eV), ^1S (ionization threshold at 49.3 eV), and $1s^2 2s 2p^3\ ^5S$ (ionization threshold at 48.3 eV) metastable terms is given in Table 1. For O^{3+}, 84% of the ions were estimated to be in the $1s^2 2s^2 2p\ ^2P$ ground term (ionization threshold at 77.3 eV), and 16% in the $1s^2 2s 2p^2\ ^4P_{1/2,\ 3/2,\ 5/2}$ metastable terms (ionization threshold at 68.8 eV). For O^{4+}, 50% of the parent ions were in the $1s^2 2s^2\ ^1S$ ground state (ionization 113.8 eV), and 50% in the $1s^2 2s 2p\ ^3P$ metastable term (ionization threshold at 103.7 eV), respectively.

3. THEORY

To interpret our experimental data, we performed MCDF calculations using the code developed by J. Bruneau (1984). For photoexcitation cross sections of O^{2+}, we included 1532 levels constructed from the 60 following configurations: $[2s2p]^4$, and $[2s2p]^3 nl$. For O^{3+}, we considered 985 levels issued from the 84 configurations $[2s2p]^3$, and $[2s2p]^2 nl$. For O^{4+}, 265 levels were included from the 45 following configurations: $[2s2p]^2$, $[2s2p]nl$. For O^{2+} and O^{4+}, $3 \leqslant n \leqslant 9$ and $0 \leqslant l \leqslant 2$, for O^{3+}, n goes up to 11. For each ionic stage, photoexcitation cross sections from the ground and the first excited levels have been computed assuming Lorentzian profiles for the shape of all excitation lines present in the experimentally investigated photon energy

range. Then, the theoretical results were convolved with the instrumental function with a constant value of 0.25 eV for the full width at half-maximum. This value corresponds to the average spectral resolution. To calculate the direct photoionization cross sections, we considered the following configurations: $[2s2p]^x$, $[2s2p]^{(x-1)}$, where x equals 4, 3, and 2 for O^{2+}, O^{3+}, and O^{4+} ions, respectively. For each level constructed on the $[2s2p]^x$ configurations, we calculated the photoionization cross sections at regular intervals on the photon energy scale (typically every 5 eV). The first energy was chosen near the ionization threshold and the last one 30 eV above. Then, the cross section was fitted to a $A(I/h\nu)^B$ law, where I is the threshold energy. A and B are the adjustable parameters of the fit. For both photoexcitation and photoionization cross sections, we used the length form of the electric-dipole operator. For each initial level, we calculated the total photoionization cross section as a sum of the photoexcitation and photoionization cross sections, i.e., without taking account any possible interference term. To compare our theoretical results with our experimental spectra, we constructed a synthetic spectrum as a weighted sum of individual total photoionization cross sections.

To further improve the previous ***R***-matrix calculations (Nahar 1998), we introduced the relativistic Breit-Pauli interaction in the Hamiltonian. Photoionization cross sections were obtained in an ab initio manner using the close-coupling (CC) approximation and ***R***-matrix method, as in the Opacity Project and Iron Project work. In the ***R***-matrix CC approximation the total wavefunction of the $(N+1)$-electron ion is represented by the wavefunctions of the N-electron core, termed as the target multiplied by the wavefunction of the outer electron as

$$\Psi_E(e+\text{ion}) = A\sum \chi_i(\text{ion})\Theta_i + \sum \chi_i \Phi_j(e+\text{ion}) \ , \qquad (1)$$

where χ_i is the target wavefunction in a specific state $S_iL_i\pi_i$ or level $J_i\pi_i$ and Θ_i is the wavefunction for the $(N+1)$-th electron in a channel labeled$S_iL_i(J_i)\pi_i k_i^2 l_i(J\pi)$; k_i^2 is its incident kinetic energy; Φ_j is the correlation function of the $(N+1)$-electron system that accounts for short-range correlations and the orthogonality between the continuum and the bound orbitals. The complex resonant structures in photoionization are included through channel coupling.

The relativistic Hamiltonian in Breit-Pauli ***R***-matrix (BPRM) method is

$$H_{N+1}^{\text{BP}} = H_{N+1} + H_{N+1}^{\text{mass}} + H_{\text{N+1}}^{\text{Dar}} + H_{N+1}^{\text{so}} \ , \qquad (2)$$

where H_{N+1} is the nonrelativistic Hamiltonian,

$$H_{N+1} = \sum\left(-\nabla_i^2 - 2Z/r_{\text{i}} + \sum 2/r_{ij}\right) \ , \qquad (3)$$

and the additional terms represent the one-body mass correction, the Darwin, and the spin-orbit interaction terms, respectively.

Photoionization cross sections for O^{2+}, O^{3+}, and O^{4+} were obtained using the same wavefunctions as in Nahar (1998). Calculations were carried out both in nonrelativistic LS coupling and in relativistic BPRM approximation. The results indicate that introduction of the relativistic effects do not significantly change the values of the continuum cross sections for these ions. Channel couplings in fine structure, however, are crucial for the metastable terms of O^{2+} and O^{3+}.

The wavefunction expansion for O^{2+} consists of 23 states of O^{3+} of configurations $2s^22p$, $2s2p^2$, $2p^3$, $2s^23s$, $2s^23p$, $2s^23d$, $2s2p3s$, and $2s2p3p$. However, the $^5S^o$ level of O^{2+} was treated with a wavefunction expansion of 15 levels of core O^{3+} of configurations $2s^22p$, $2s2p^2$, and $2p^3$. The wavefunction for O^{3+} consists of a 20-level expansion of the core ion O^{4+} with configurations $2s^2$, $2s2p$, $2p^2$, $2s3s$, $2s3p$, and $2s3d$. The wavefunction expansion for O^{4+} consists of nine states of core O^{5+} of configurations $1s^22s$, $1s^22p$, $1s^23s$, $1s^23p$, $1s^23d$, $1s^24s$, $1s^24p$, $1s^24d$, and $1s^24f$. More details will be provided in a separate publication. Computations were extensive as very fine energy resolution, varying with resonances, was required to delineate the features of the resonances and to obtain the narrow resonances which are easy to miss. To compare directly the theoretical results with the experimental spectra, we used the same procedure as the one applied to the MCDF results, keeping, however, the weight of each term as determined from the MCDF calculations. In this paper, the energy scales of our ***R***-matrix results were adjusted to the experimentally measured threshold energies of the ground state for each ion.

4. RESULTS

The measured cross section for single photoionization of O^{2+} ions is presented in the upper part of Figure 1. The relative variation of the single photoionization cross section results from the measurement of the O^{3+} signal over the 46–80 eV photon energy range. The relative cross section scale was made absolute by normalization to the data resulting from our measurements of the absolute photoionization cross section at 56.2 eV ($\sigma = 3.18 \pm 0.45$ Mbarn) and 68.3 eV ($\sigma = 2.48 \pm 0.42$ Mbarn) photon energies, i.e., at photon energies where the cross section is varying smoothly. Steps corresponding to the ionization thresholds for $^1D_2$ and $^3P_{0,1,2}$ terms can be seen near 51.9 eV and at 54.81 eV, respectively. In Table 2, we summarize, for O^{2+}, as well as

TABLE 2

MEASURED AND CALCULATED VALUES OF THE IONIZATION THRESHOLDS IN O^{2+}, O^{3+}, AND O^{4+} IONS

Ion	Ionization Threshold	Experiment	MCDF	NIST[a]
O^{2+}	$1s^22s2p^3\ ^5S_2$		47.13	47.397
	$1s^22s^22p^2\ ^1S_0$		48.30	49.522
	$^1D_2$		50.79	52.306
	$^3P_{0,1,2}$	54.81 (8)	53.66	54.876
	$1s^22s2p^3\ ^5S_2\rightarrow$			
	$\rightarrow[(1s^22s2p^2\ ^4P)+\varepsilon l]\ O^{3+}$	56.22 (8)[b]	55.56	56.27
O^{3+}	$1s^22s2p^2\ ^4P_{5/2}$		67.91	68.49
	$^4P_{3/2}$		67.84	68.51
	$^4P_{1/2}$		67.82	68.54
	$1s^22s2p\ ^2P_{3/2}$	77.20(10)	76.31	77.36
	$^2P_{1/2}$		76.36	77.41
	$1s^22s2p^2\ ^4P\rightarrow$			
	$\rightarrow[(1s^22s2p\ ^3P)+\varepsilon l]\ O^{4+}$	78.73(3)[b]	78.20	78.64
O^{4+}	$1s^22s2p\ ^3P_{0,1,2}$	103.50(5)	103.31	103.73
	$1s^22s^2\ ^1S_0$	113.66(13)	113.54	
	$1s^22s2p\ ^3P\rightarrow$			$113.89\ ^2S$
	$\rightarrow[(1s^22s\ ^2S)+\varepsilon l]\ O^{5+}$	115.46(5)[b]	115.43	$115.93\ ^2P$

NOTE.—Energies are in eV.

[a] From the table published by Moore 1993.

[b] Determined using the measured value of the quantum defect for the Rydberg series converging to this ionization threshold.

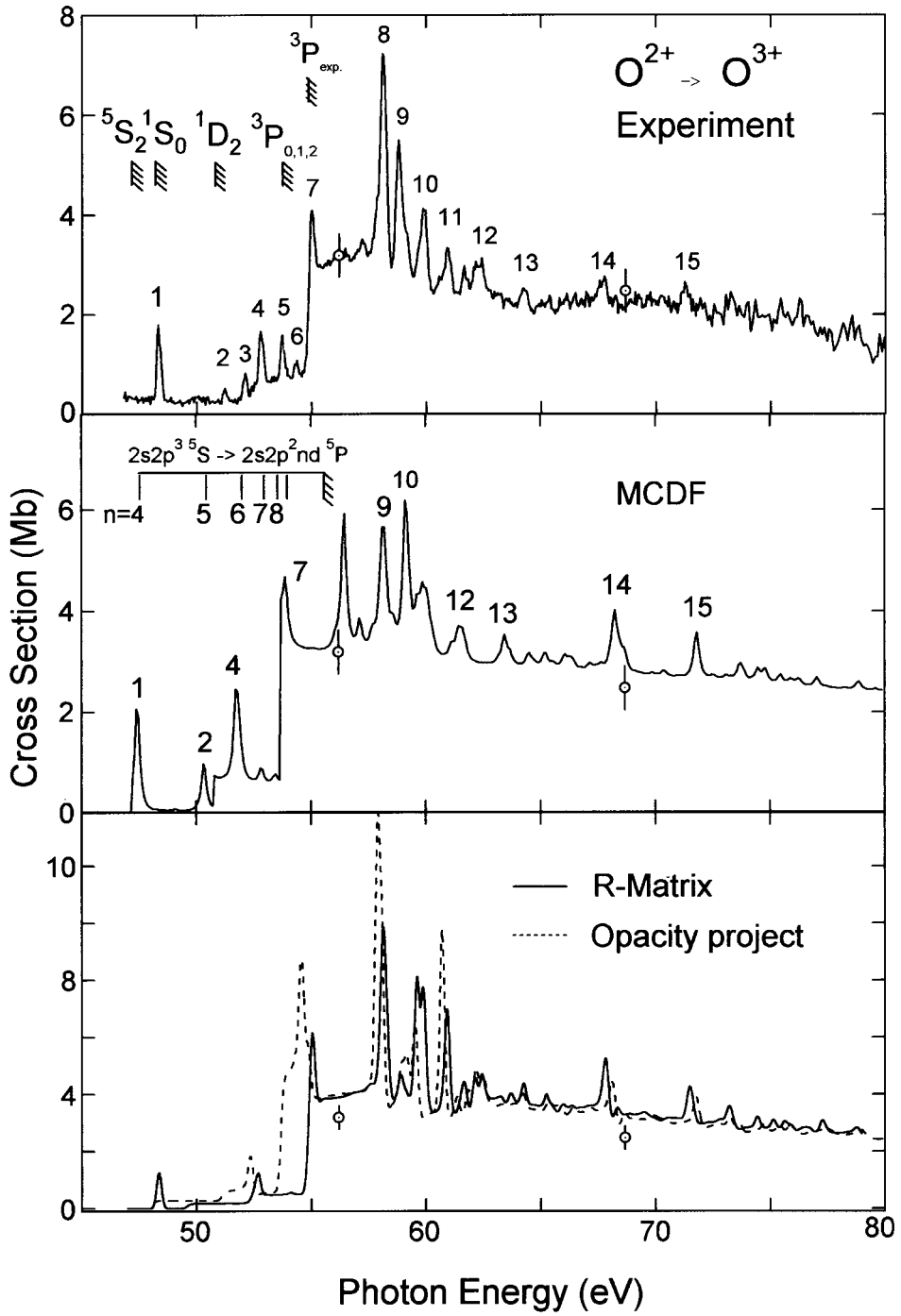

FIG. 1.—Variation of the single photoionization cross section of O^{2+} ions over the 46–80 eV photon energy range. *Upper panel*: experimental results. The position of the energies of the experimental ionization thresholds are marked by vertical-dashed lines. The first members of the $1s^22s2p^3\ ^5S \rightarrow 1s^22s2p^2nd\ ^5P$ Rydberg series and the resonance lines above the ground state threshold are labeled by numbers. The two points shown with error bars are the measured normalization values of the absolute cross section scale. *Middle panel*: results of our MCDF calculations. The two absolute cross section values are again shown for easier comparison with theory. *Bottom panel*: results of the present ***R***-matrix calculations in the Opacity Project (*dashed line*) and of the new ***R***-matrix calculations (this work). In this figure, as well as in Figs. 2 and 3, all synthetic spectra have been convoluted with the instrumental function (FWHM = 0.25 eV). It should be noted that the ordinate scale is not the same for the ***R***-matrix results as for the MCDF and experimental results.

for O^{3+} and O^{4+}, the experimental and MCDF values of the $2p$-ionization thresholds, and the $2s$-ionization thresholds for O^{4+}. For $O^{2+}$and O^{3+} ions, there is a systematic difference of -0.7 to -1 eV for the calculated energies values as compared with our experimental measurements. For O^{4+} ions, the calculated energies are slightly lower than but in closer agreement with the measured values (in average -0.25 eV). Values available in the NIST tables (Moore 1993, p. 336) are also given for comparison.

The Rydberg series of resonances corresponding to outer shell excitation of a $2p$-electron from the $1s^22s2p^3\ ^5S$ metastable term to the $1s^22s2p^2nd\ ^5P$, ^5D autoionizing terms is clearly seen below the $^3P_{0,1,2}$ ionization thresholds. The first member of the series seen here, assigned to the $2p \rightarrow 4d$

TABLE 3
ENERGIES AND ASSIGNMENT OF THE RESONANT STRUCTURES OBSERVED IN PHOTOIONIZATION OF O^{2+} IONS

Peak Number	*nl*	Experiment	MCDF	MCDF Transitions[a]
1	4*d*	48.29 (17)	47.54	$1s^2 2s 2p^3\ ^5S_2 \rightarrow 1s^2 2s 2p^2\ 4d\ ^5P_{1,2,3}$
2	5*d*	51.17 (15)	50.42	$5d\ ^5P_{1,2,3}$
4	6*d*	52.75 (12)	51.91	$6d\ ^5D_{1,2,3}$
			52.00	$6d\ ^5P_{1,2,3}$
5	7*d*	53.68 (10)	52.91	$7d\ ^5D_{1,2,3}$
			52.94	$7d\ ^5P_{1,2,3}$
6	8*d*	54.27 (13)	53.52	$8d\ ^5D_{1,2,3}$
			53.55	$8d\ ^5P_{1,2,3}$
	9*d*		53.960	$9d\ ^5D_{1,2,3}$
			53.968	$9d\ ^5P_{1,2,3}$
7	4*p*	54.98 (16)	53.60	$1s^2 2s^2 2p^2\ ^3P \rightarrow 1s^2 2s 2p^2\ 4p\ ^3D_{1,2,3}$
8	5*p*	57.15 (16)	56.56	$5p\ ^3D_{1,2,3}$
9	6*p*	58.06 (23)	57.40	$6p\ ^3D_{1,2,3}$
10	7*p*	59.81 (28)	59.22	$7p\ ^3D_{1,2,3}$
11		60.86 (23)	60.11	$1s^2 2s^2 2p^2\ ^3P_{0,1} \rightarrow 3p/4p\ ^3P_{1,2}$
13		64.18 (24)	63.66	$1s^2 2s^2 2p^2\ ^1S_0 \rightarrow 3p/4p\ ^1P_1$

NOTE.—Energies are in eV.
[a] These assignments refer to the transitions having the highest calculated oscillator strengths.

transition, is labeled 1 in the figure. Upper members of the series are peaks labeled 2 ($n = 5$), 4 ($n = 6$), 5 ($n = 7$), and 6 ($n = 8$). The measured energies of these resonances are given in Table 3, together with our MCDF calculated values. As for the ionization threshold values, the MCDF results are lower than the experimental measurements, by about 0.8 eV. Peak 3 does not belong to the series and has not yet been identified. The series converges to the $1s^2 2s 2p^2$ ionization thresholds near 63.31 eV, i.e., 8.5 eV above the $^3P_{0,1,2}$ thresholds, as deduced from our measured excitation energies. The value of the quantum defect for this series was found to be low, at about 0.10 ± 0.05, in good agreement with the results of our MCDF calculations. The very low value of the averaged quantum defect for this series means that the nuclear charge is almost fully screened—for an outer electron excited to an *nd* orbital ($n \geqslant 4$)—by the inner electrons in the $n = 1$ and $n = 2$ shells. The relative intensities of the members of the series, however, are strongly perturbed and do not follow the usual $1/n^*3$ rule (Condon & Shortley 1935).

A strong resonance, peak 7, is visible just at the energy of the $^3P_{0,1,2}$ ionization thresholds. From our MCDF calculations, we attribute it to the transitions $1s^2 2s^2 2p^2\ ^3P_{0,1,2} + h\nu \rightarrow 1s^2 2s 2p^2 4p\ ^3D_{1,2,3}$ experimentally measured at 54.98 eV excitation energy (against an MCDF calculated value of 53.60 eV). The overlap of peak 7 with the ionization threshold may explain why its theoretical energy is lower in the calculations than the measured value by as much as 1.40 eV. The higher members of this series (excitation $2s \rightarrow np$) are listed also in Table 2, together with the MCDF results. Above peak number 10, the assignment of transitions corresponding to peaks 11–15 is very tentative, as each of these peaks results evidently from several different transitions. The proposed assignments, however, are consistent with the averaged shift of −0.65 eV for the MCDF energies.

Our absolute experimental data are compared, in the middle of Figure 1, to the results of our MCDF calculations. In addition to the almost constant energy shift, the theoretical spectrum shows some differences between the relative intensities of the measured and calculated resonant structures. Above 60 eV, both experimental and theoretical spectra have the same general behavior.

In the lower part of Figure 1, we show the results of our new ***R***-matrix calculations of the photoionization cross section, together with the ***R***-matrix results extracted from the Opacity Project database. First, there are significant differences between the two ***R***-matrix calculations. One can note, in particular, strong changes in the intensities of the most intense resonances. The calculated values of the $^3P_{0,1,2}$ ionization thresholds are also significantly different, with the results from the most recent calculations being the closest to the experimental value. This can be understood, as the latest calculations include a higher number of states to represent the target. There are, however, some differences between our experimental and the latest ***R***-matrix calculated spectra. The $^5S \rightarrow {}^5P$ Rydberg series is now present in the results of the theoretical calculation since it has been performed in the relativistic approximation. Due to spin conservation, the photoexcited level cannot decay in LS coupling to the ground $2s^2 2p\ ^2P$ configuration. Performing ***R***-matrix calculations in the relativistic approximation has, indeed, been recently shown to be necessary to understand the fine structure of the photoionization spectrum for C^+ ions (Nahar 2002). The Rydberg series below the main ionization threshold shows up with a high number of very narrow lines in our ab initio calculation. All of them are mainly due to fine-structure mixing of the ^5P term. Taking into account the small percentage of atoms in the ^5S metastable term, the convolution procedure, however, reduces considerably the number of Rydberg lines that are finally visible; in fact, only one line, calculated near 48.5 eV, can be seen in the convoluted theoretical result (None of them are present in the theoretical results calculated neither in the Opacity Project nor in the 1998 calculations, since these calculations have been performed in the nonrelativistic approximation).

The calculated intensity distribution among the first resonant transitions at and above the $^3P_{0,1,2}$ ionization thresholds differs from the experimental data. Higher experimental resolution would be needed for a more detailed comparison between the experiment and the MCDF and

TABLE 4
COMPARISON OF EXPERIMENTAL AND THEORETICAL CROSS SECTION VALUES FOR O^{2+} AND O^{3+} OVER THE 56–90 eV ENERGY RANGE

Photon Energy (eV)	Experiment[a] (Mbarn)	DS[b] (Mbarn)	MCDF[a] (Mbarn)	*R*-Matrix[a] (Mbarn)
		O^{2+}		
56	3.2 (6)	3.8	3.5	4.0
60	3.0 (5)	3.3	3.4	3.8
65	2.7 (5)	2.8	3.2	3.4
70	2.4 (4)	2.4	3.1	3.1
75	2.1 (7)	2.1	2.9	2.8
80	1.8 (4)	1.8	2.8	2.5
		O^{3+}		
79	2.1 (4)[c]	1.12	1.29	0.76
85		0.93	1.07	
90	1.5 (2)	0.81	1.48	
95	1.4 (2)	1.62	1.33	2.10
100	1.1 (2)	1.46	1.50	

NOTES.—Since the Dirac-Slater ionization threshold for the ground state differs significantly from the experimental value, the theoretical values of these DS cross sections are given for the same excess energy above this threshold. The Dirac-Slater values are the calculated cross sections for the ions in the ground state.
[a] This work.
[b] Dirac-Slater, Verner et al. 1993
[c] Value likely modified by a resonance located near this photon energy.

R-matrix calculations. The absolute values of the experimentally measured cross section differs from the calculated values by about 30% for the *R*-matrix calculations (the theoretical values being too high) and by less than 20% for the MCDF calculations (i.e., the MCDF-values stay within the experimental uncertainty). A more detailed comparison is made in Table 4, where we give the results of the various theoretical calculations of the photoionization cross section for O^{2+} (and also for O^{3+}) in comparison with our measured values. Such a discrepancy with the *R*-matrix calculations has already been noted for photoionization of C^+ (Kjeldsen et al 2002), but for O^+ (Covington et al. 2001) the *R*-matrix calculated cross section is lower than the measured cross section. Surprisingly enough, the single-configuration Dirac-Slater (DS) results (Verner et al. 1993) are the closest to the experimental values.

Our experimental results for single photoionization of O^{3+} are shown in the upper part of Figure 2. The relative variation of the single photoionization cross section results from the measurement of the O^{4+} signal from 67 to 100 eV. The relative cross section scale was made absolute by normalization to the data resulting from our measurements of the absolute photoionization cross section at 79 eV ($\sigma = 2.07 \pm 0.38$ Mbarn), i.e., just above the ionization thresholds of the ground state. A step corresponding to the ionization thresholds of the ground state ($1s^2 2s^2 2p\ ^2P_{1/2,3/2}$) states is seen at 77.2 eV (see Table 2 for a list of the various measured and calculated ionization thresholds). Our results are rather similar to the results previously shown in the case of O^{2+}. The interpretation of the spectrum is simple below the ground state ($1s^2 2s^2 2p\ ^2P_{1/2,3/2}$) ionization thresholds, i.e., below 77.2 eV. Resonances measured over this energy range are due to outer shell excitation of a $2p$-electron from the $1s^2 2s 2p^2\ ^4P_{1/2,3/2}$ metastable levels to the $1s^2 2s 2pnd\ ^4P$, ^4D excited terms (electronic transition $2p \rightarrow nd$, $n \geqslant 5$). Seven members (peaks 1–7) of the series, from the $1s^2 2s 2p 5d$ level at 70 eV photon energy up to the $1s^2 2s 2p 11d$ level, at 77 eV, just below the ionization threshold of the ground state at 77.2 eV, are very clearly seen, with an excellent signal-to-noise ratio. The measured energies of these resonances are given in Table 5, together with the results of our MCDF calculations, which show the same systematic shift between the MCDF-values and the experimental values (in average -0.58 eV) as in the case of O^{2+}. The series converges to the $1s^2 2s 2p\ ^3P$ ionization threshold, at about 78.7 eV, as deduced from the measured values of our resonance energies, using the measured values of the quantum defect (see Table 2). The quantum defect for this series is equal to 0, confirming that higher is the charge of the oxygen ion, closer

TABLE 5
ENERGIES AND ASSIGNMENT OF THE RESONANT STRUCTURES OBSERVED IN PHOTOIONIZATION OF O^{3+}

Peak Number	*nl*	Exp. Energy	MCDF Energy	MCDF Transitions[a]
1	$5d$	69.75 (6)	69.18	$1s^2 2s 2p^2\ 4P_{1/2,3/2,5/2} \rightarrow 1s^2 2s 2p\ 5d\ ^4P, ^4D$
2	$6d$	72.54 (6)	71.94	$6d$
3	$7d$	74.22 (6)	73.60	$7d$
4	$8d$	75.27 (7)	74.68	$8d$
5	$9d$	75.96 (6)	75.41	$9d$
6	$10d$	76.48 (6)		$10d$
7	$11d$	76.91 (6)		$11d$
8	$5p$	78.12 (6)	77.39	$1s^2 2s^2 2p\ ^2P_{1/2,3/2} \rightarrow 1s^2 2s 2p 5p\ ^2P_{1/2,3/2}\ ^2D_{3/2,5/2}$
9	$5p$	79.49 (7)	77.58	$5p\ ^2S_{1/2}$
10	$6p$	80.14 (9)	80.30	$6p\ ^2S\ ^2P\ ^2D$
11	$4d$	81.27 (6)	81.43	$1s^2 2p^2 4d\ ^2D_{3/2,5/2}$
12	$7p$	82.82 (6)	81.98	$1s^2 2s 2p 7p\ ^2S\ ^2P\ ^2D$
13	$8p$	83.94 (6)	83.09	$8p\ ^2P\ ^2D$
14	$9p$	84.72 (6)	83.88	$9p\ ^2P\ ^2D$
15		85.37 (7)		
16		85.70 (7)		
17		87.14 (7)		
18		90.51 (6)		

NOTE.—Energies are in eV.
[a] These assignments refer to the transitions having the highest calculated oscillator strength.

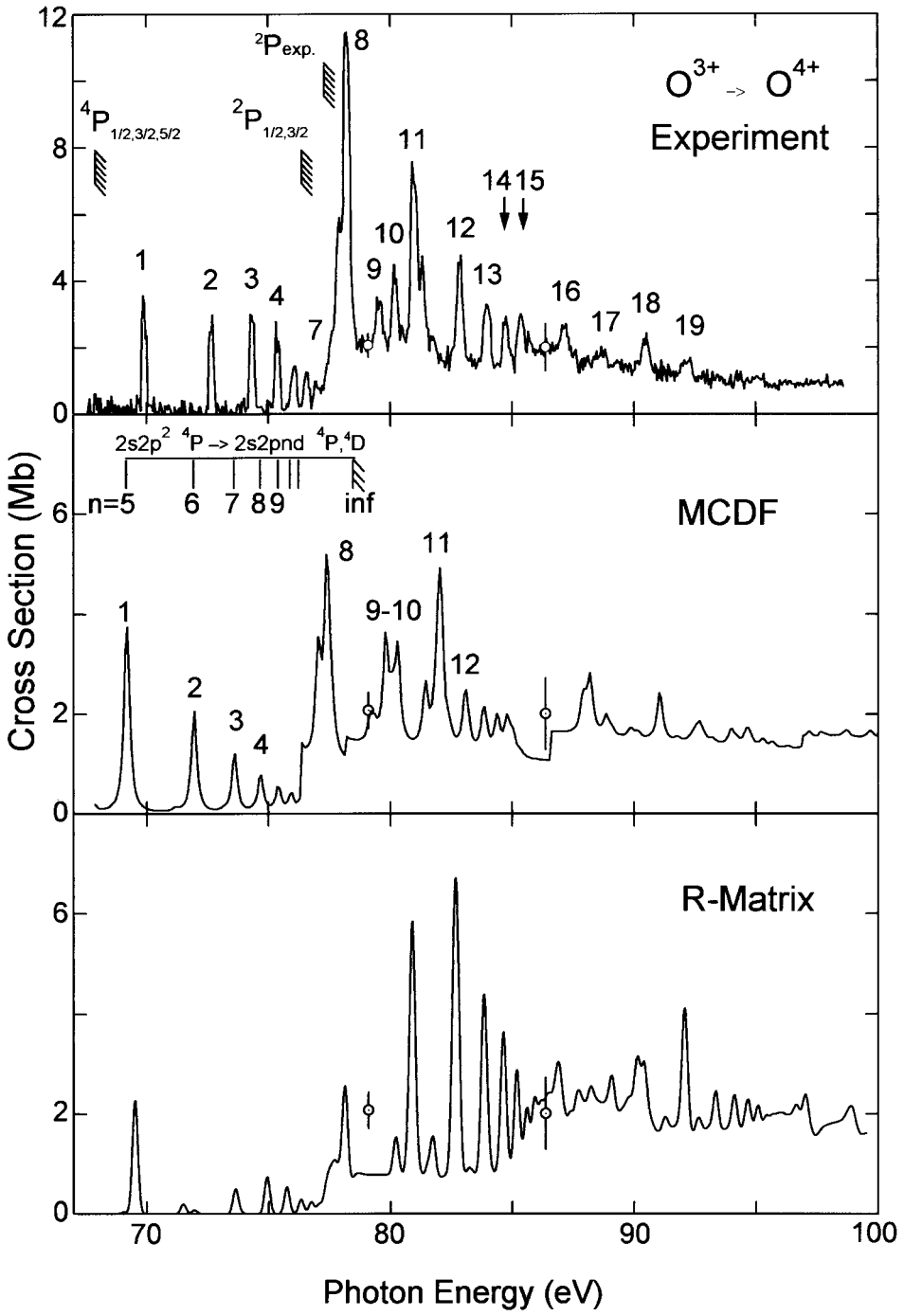

FIG. 2.—Variation of the single photoionization cross section of O^{3+} ions over the 67–99 eV photon energy range. *Upper panel*: experimental results. The position of the energies of the experimental ionization thresholds are marked by vertical dashed lines. The first members of the $1s^22s2p^2\,{}^4P \rightarrow 1s^22s2pnd\,{}^4P, {}^4D$ Rydberg series are visible below the ground state threshold (lines 1–7). The point shown with error bars at 79 eV is the measured normalization value of the absolute cross section scale. *Middle panel*: results of our MCDF calculations. The value of the absolute cross section experimentally measured at 79 eV is also shown for easier comparison with theory. *Bottom panel*: results of the present ***R***-matrix calculations after convolution with the instrumental function (FWHM = 0.25 eV). Here the ordinate scale for both theoretical results is not the same as for the experimental results.

to a hydrogenic behavior is the nuclear potential seen by the outer electron. The relative intensities of the members of this series show also an irregular behavior.

A strong resonant doublet peak, labeled 8 in the figure, is overlapping with the $^2P_{1/2,3/2}$ ionization threshold at 78 eV. It is due to the excitation of a 2*s*-electron onto an *np* orbital according to $1s^22s^22p\ {}^2P_{1/2,3/2} \rightarrow 1s^22s2p5p\ [{}^2P_{1/2,3/2} + {}^2D_{3/2,5/2}]$. The MCDF energy value is, again, shifted by −0.73 eV from the experimental value. Higher members of this series show up between 80 and 84 eV, but an accurate assignment of the experimentally observed resonances is made difficult by the high possible numbers of excited states revealed by our MCDF calculations.

Our absolute experimental data are compared, in the middle and lower panels of Figure 2, with the results of our MCDF and the ***R***-matrix calculations, respectively. The resonant structures due to the excitation of the metastable states are nicely reproduced by our MCDF results, as well

as by the ***R***-matrix calculations. The relative intensities of the resonance lines observed below the ionization threshold of the ground state in the simulated MCDF and ***R***-matrix spectra are, however, different from the ones experimentally measured for this Rydberg series. Above the $^2P_{1/2,3/2}$ ionization thresholds none of the theoretical results are in quantitative agreement with the experimental spectrum, although the general behavior of the cross section is correctly reproduced over the resonant energy region. The absolute values of the theoretical cross section are compared in Table 4 with the measured cross sections. Above the main ionization threshold, at a photon energy of 79 eV, the experimental cross section is in good agreement with the MCDF calculations but does not agree with the calculated ***R***-matrix results. In particular, the experimental slope of the cross section shows continuously decreasing values of the experimental cross section up to 100 eV photon energy, in agreement with the MCDF results. Between the main ^2P ionization thresholds and the opening of the $1s^22s2p\varepsilon$l continuum of O^{4+} (around 86 eV), the ***R***-matrix calculations are in significant discrepancy with the experimental data. Above the opening of this channel up to 100 eV, there is a relatively good agreement between ***R***-matrix and experimental results.

The results of our experiments for single photoionization of O^{4+} ions between 95 and 130 eV photon energies is shown in the upper panel of Figure 3. For this highly charged ion, we present only relative cross section measurements since the O^{5+} signal was too small to allow accurate enough absolute measurements. Two steps are distinctly visible in the spectrum. The first step is measured at the ionization threshold of the $1s^22s2p\ ^3P_{0,1,2}$ metastable term of O^{4+}, the second one is seen at the ionization threshold of the $1s^22s^2\ ^1S_0$ ground state of O^{4+} (see Table 2 for the experimental and theoretical values of the ionization thresholds). A first series of resonances is seen between the two ionization thresholds. It is due to a $2s\rightarrow np$ excitation from the $1s^22s2p\ ^3P_{0,1,2}$ metastable term. Since the O^{4+} ion in these unresolved metastable states is helium-like when one considers only the two outer electrons attracted by a (2+) nuclear charge, there might be a strong mixing of *ns* and *np* states, and the possible excited states can be determined like in the case of helium (Cooper, Fano, & Pratts 1963), which means than there is a large number of such excited states. Four members of this Rydberg series, labeled as peaks 1–4 ($n = 6$–9) are observed in Figure 3. In Table 6, we give the measured values of the resonance energies, experimentally measured and theoretically calculated using our MCDF code, as well as the proposed identifications of the resolved transitions. The MCDF-values are lower than the experimental results by about 0.10 eV. The measured quantum defect of this series is 0.10 ± 0.10. This series converges to the $1s^22s\ ^2S$ level of O^{5+} at a theoretical MCDF energy value of 115.43 eV, as marked in the figure, in good agreement with the experimental value (115.46 eV, determined from the quantum defect). This series is well reproduced by our MCDF calculations as shown in the middle panel of Figure 3 as well as in Table 5. The results of the ***R***-matrix calculations presented in the lower panel of Figure 3 show also members of this Rydberg series, but the experimentally measured relative intensities are far from being reproduced by these calculations. Above the ^1S ionization threshold, the experimental spectrum is too noisy to allow nonambiguous observation of individual resonance lines but for the single one measured at 116.24 eV (peak 5 in the figure). Our MCDF calculations predict the first member ($n = 6$) of the $1s^22s^2\ ^1S_0\rightarrow 1s^22pnd\ ^1P_0$ double-excitation Rydberg series to be at an energy of 116.39 eV, in relatively good agreement with the experimental measurement (the theoretical shift is negligible). The predicted energies of the next members of this series are also given in Table 6. It is interesting to note that the measured intensity of the first members of this second Rydberg series is significantly lower than the ones of the first series, which could be expected since two-electron transitions are likely to be less intense than single excitation transitions.

5. CONCLUSION

To conclude, we summarize the main results of our experiments and calculations. For the three ions, O^{2+}, O^{3+}, and O^{4+}, a strong contribution to resonant photoionization from the metastable states is clearly observed and theoretically confirmed by our MCDF and ***R***-matrix calculations, indicating that, even for these light ions, a relativistic treatment is sometimes needed to correctly describe the observed autoionizing structures. The energies of the members of these O^{q+} series as well as the ionization thresholds are well reproduced by our MCDF calculations, within a maximum shift of -1 eV for O^{2+} and O^{3+}, and -0.10 eV for O^{4+}, respectively. Resonant structures, due to excitation of the ground state of these ions, are also measured above the ground state ionization thresholds, but the agreement with the results of our MCDF and the ***R***-matrix calculations is only qualitative, owing to the large number of possibly involved transitions. For O^{2+}, our MCDF and ***R***-matrix calculations give values of the cross sections that are higher

TABLE 6
ENERGIES AND ASSIGNMENT OF THE RESONANT STRUCTURES OBSERVED IN PHOTOIONIZATION OF O^{4+}

Peak Number	*nl*	Exp. Energy	MCDF Energy	MCDF Transitions[a]
1	6*p*	105.65 (12)	105.55	$1s^22s2p\ ^3P_{0,1,2}\rightarrow 1s^22p\ 6p\ ^3D_{1,2,3}\ ^3P_{0,1,2}\ ^3S_1$
2	7*p*	108.29 (10)	108.20	$7p\ ^3D_{1,2,3}\ ^3P_{0,1,2}$
3	8*p*	109.97 (11)	109.90	$8p\ ^3D_{2,3}\ ^3P_{1,2}$
4	9*p*	111.09 (21)	111.06	$9p\ ^3D_{2,3}\ ^3P_1$
5	6*d*	116.24 (15)	116.39	$1s^22s^2\ ^1S_o\rightarrow 1s^22p6d\ ^1P_1$
	7*d*		118.83	7*d*
	8*d*		120.42	8*d*
	9*d*		121.52	9*d*

NOTE.—Energies are in eV.
[a] These assignments refer to the transitions having the highest calculated oscillator strengths.

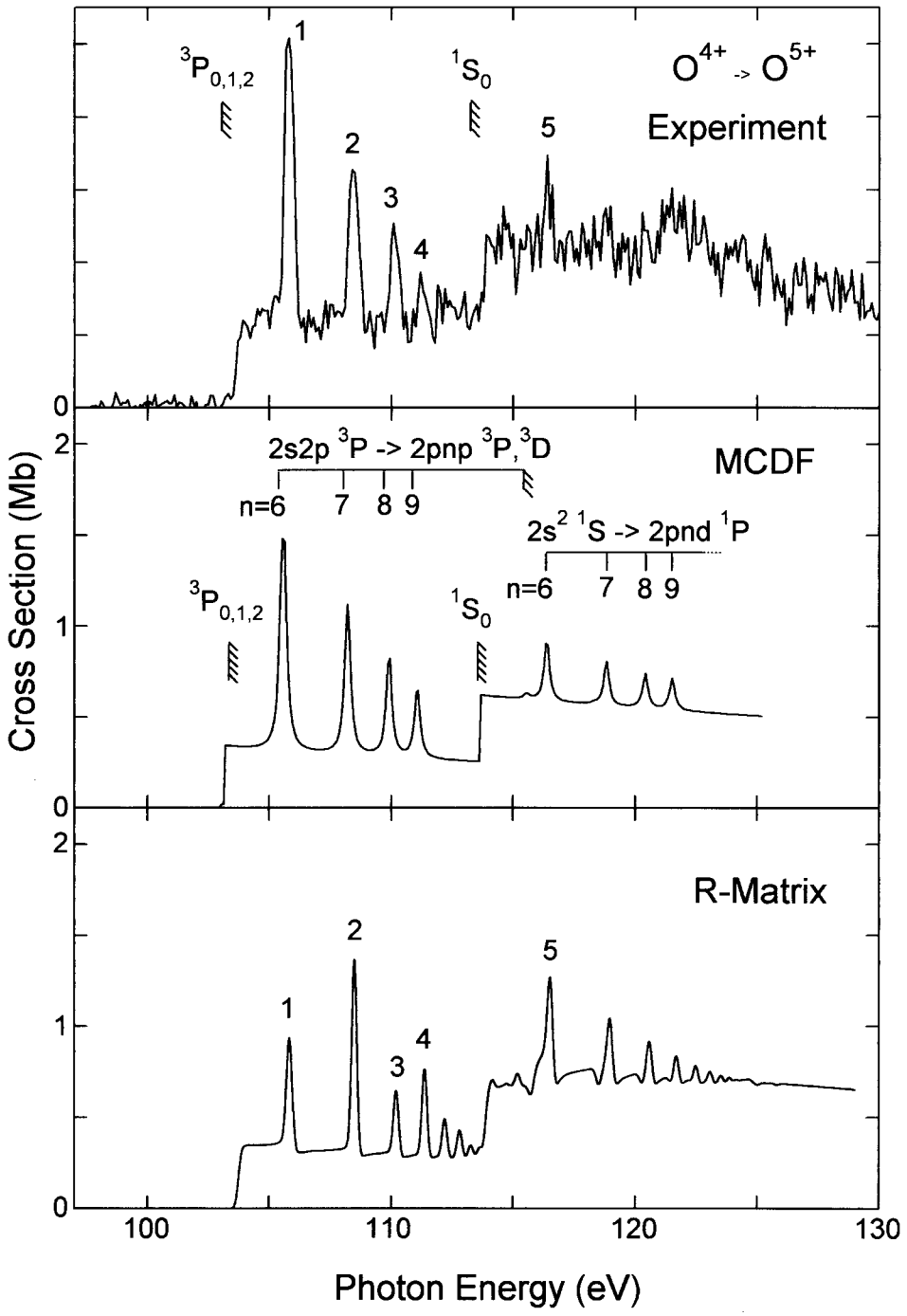

FIG. 3.—Variation of the single photoionization cross section of O^{4+} ions over the 95–130 eV photon energy range. *Upper panel*: experimental results. The position of the energies of the experimental ionization thresholds are marked by the vertical-dashed lines. The first members of the $1s^22s2p\ ^3P \rightarrow 1s^22pnp\ ^3P, ^3D$ Rydberg series (lines 1–4) are clearly visible below the ground state ionization threshold. *Middle panel*: results of our MCDF calculations. The relative intensities of the Rydberg lines due to excitation of the metastable state are in good agreement with the results of the experiment. *Bottom panel*: results of the present ***R***-matrix calculations after convolution with the instrumental function (FWHM = 0.25 eV). The Rydberg series shows up very nicely, with nonregular distribution of the relative intensities, however.

than the measured ones, while the best agreement is obtained with the single-configuration Dirac-Slater calculation. For O^{3+}, over the energy range extending up to 10 eV above the main ionization threshold, the MCDF results are in good agreement with the experimental results, while the ***R***-matrix values are significantly lower. At higher photon energy, both MCDF and ***R***-matrix simulated spectra agree well with the measured experimental cross section. Further insight into the knowledge of the photoionization spectra of multiply charged oxygen ions should be provided by the access to synchrotron facilities providing higher brightness photon beams.

REFERENCES

Bevington, P. R. 1969, Data Reduction and Error Analysis for the Physical Sciences (New York: McGraw-Hill)
Bizau, J.-M., et al. 2000, Phys. Rev. Lett., 84, 435
———. 2001, Phys. Rev. Lett., 87, 273002
———. 2003, Nucl. Instrum. Meth. B, 205, 290
Bruneau, J. 1984, J. Phys. B, 17, 3009
Burke, V. M., Lennon, D. J., & Seaton, M. J. 1989, MNRAS, 236, 353
Condon, E. U., & Shortley, G. H. 1935, The Theory of Atomic Spectra (Cambridge Univ. Press)
Cooper, J. W., Fano, U., & Pratts, R. 1963, Phys. Rev. Lett., 10, 518
Covington, A. M., et al. 2001, Phys. Rev. Lett., 87, 243002
Cunto, W., Mendoza, C., Ochsenbein, F., & Zeippen, C. J. 1993, A&A, 275, L5
Kjeldsen, H., Folkmann, F., Hansen, J. E., Knudsen, H., Rasmussen, M. S., West, J. B., & Andersen, T. 1999, ApJ, 524, L143
Kjeldsen, H., Kristensen, B., Brooks, R. L., Folkmann, F., Knudsen, H., & Andersen, T. 2002, ApJS, 138, 219
Kjeldsen, H., West, J. B., Folkmann, F., Knudsen, H., & Andersen, T. J. 2000, J. Phys. B, 33, 1403
Lyon, I. C., Peart, B., West, J. B., & Dolder, K. 1986, J. Phys. B, 19, 4137
Moore, C. E. 1993, Handbook of Chemistry and Physics (Boca Raton: CRC Press)
Müller, A., et al. 2002, J. Phys. B, 35, L137
Nahar, S. N. 1998, Phys. Rev. A, 58, 3766
———. 2002, Phys. Rev. A, 65, 052702
Nahar, S. N., & Pradan, A. K. 1994, Phys. Rev. A, 49, 1816
Nasreen, G., Deshmukh, P. C., & Manson, S. T. 1988, J. Phys. B, 21, L281
Oura, M., et al. 2001, Phys. Rev. A, 63, 014704
Peart, B., & Lyon, I. C. 1987, J. Phys. B, 20, L673
Reilmann, R. F., & Manson, S. T. 1979, ApJS, 10, 815
Verner, D. A., Yakovlev, D. G., Band, I. M., & Trzhaskovskaya, M. B. 1993, At. Data Nucl. Data Tables, 55, 233
West, J. B. 2001, J. Phys. B, 34, 45